Journal of Molecular Graphics and Modelling 39 (2013) 50–60

Contents lists available at SciVerse ScienceDirect

Journal of Molecular Graphics and Modelling

journal homepage: www.elsevier.com/locate/JMGM

A homology modeling study toward the understanding of three-dimensional structure and putative pharmacological profile of the G-protein coupled receptor GPR55

Orgil Elbegdorj, Richard B. Westkaemper, Yan Zhang*

Department of Medicinal Chemistry, School of Pharmacy, Virginia Commonwealth University, 800 E. Leigh Street, P.O. Box 980133, Richmond, VA 23219-1540, USA

ARTICLE INFO

Article history:
Received 8 August 2012
Received in revised form 8 October 2012
Accepted 13 October 2012
Available online 23 October 2012

Keywords:
GPR55
G-protein coupled receptors
Homology modeling
Automated docking

ABSTRACT

The orphan G-protein coupled receptor GPR55 was shown to bind to certain cannabinoid compounds which led to its initial classification as the third type of cannabinoid receptor. Later studies showed that lysophosphatidylinositol (LPI) also activated GPR55, in particular 2-arachidonoyl-LPI was proposed to be its endogenous ligand. However, the results of pharmacological studies regarding GPR55 have been quite inconsistent. Despite its contradictory pharmacological profile, GPR55 has been implicated in various disease states including inflammatory and neuropathic pain, metabolic bone diseases, and cancer. Herein, we report the ligand binding properties of GPR55 by applying homology modeling and automated docking algorithms in order to understand its pharmacological profile. The 3D homology model of GPR55 was built based on the adenosine A_{2A} receptor crystal structure. Docking studies of several types of reported ligands were carried out afterwards. The results indicated that both hydrogen bonding and hydrophobic interactions contributed significantly for its ligand binding and the amino acid residue Lys80 seemed to be the anchor residue for receptor recognition. In addition, its putative agonist and antagonist appeared to recognize different domains of the receptor corresponding to their reported pharmacological activities.

1. Introduction

G-protein coupled receptors (GPCRs) exist in most organ systems and present a wide range of opportunities as therapeutic targets in areas including cancer, cardiac dysfunction, diabetes, CNS disorders, obesity, inflammation, and pain [1]. There are still numerous orphan GPCRs with no known endogenous ligands. Targeting these orphan receptors and exploring their functions in the body may lead to novel therapeutics to treat human diseases. The orphan receptor GPR55 was first identified and cloned in 1999 [2]. Soon after, two independent patents claimed that this receptor may be the "third-type" cannabinoid receptor (CB3) [3].

Since then, GPR55 has been pharmacologically examined in transfected HEK293 cells with number of cannabinoid ligands. So far the results of these studies have been quite contradictory [4]. For example, Ryberg et al. found that GPR55 stably transfected in HEK293 cells could be activated by nanomolar concentrations of the endocannabinoids anandamide, 2-arachidonylglycerol (2-AG), and virodhamine in GTPγS functional assay. On the other hand, cannabidiol (CBD) was shown to be able to antagonize the effects of CP55940 and anandamide with an IC_{50} of 440 nM [5]. In contrast, Oka et al. found that many cannabinoid ligands including 2-AG, anandamide, CP55940, and Δ^9-THC had no effect on the intracellular calcium levels in HEK293 cells stably expressing GPR55. They proposed that 2-arachidonoyl lysophosphatidylinositol (LPI) was the endogenous ligand for GPR55 based on the fact that LPI could induce the phosphorylation of extracellular signal-regulated kinase (ERK) and rapid calcium transients in GPR55 expressing cells [6]. Besides, some other experimental evidence suggested that GPR55 coupled to G_{12} and G_{13}, which may activate small G-protein RhoA and mobilize intracellular calcium [7]. This highly contentious pharmacology in part can be explained by the concept of functional selectivity, which implies that GPR55 downstream signaling may be ligand and tissue-dependent. To be noticed, the absence of highly selective modulators and the lack of receptor structural data have hampered the progress in this particular research area. Development of potent and selective ligands for GPR55 based on the understanding of its 3D conformation will certainly be useful in answering these outstanding questions regarding its pharmacology and physiological role in the body [8].

Recently the potential role of GPR55 in analgesia was investigated using GPR55 knockout (KO) mice. Compared to GPR55 wild type mice, GPR55 KO mice failed to develop mechanical hyperalgesia following clinical models of inflammatory and

* Corresponding author.
E-mail address: yzhang2@vcu.edu (Y. Zhang).

1093-3263/$ – see front matter © 2012 Elsevier Inc. All rights reserved.
http://dx.doi.org/10.1016/j.jmgm.2012.10.005

neuropathic pain [9]. GPR55 was also found to be highly expressed in large-diameter dorsal root ganglion (DRG) neurons, which may be involved in neuropathic or inflammatory pain [10]. Another study showed that GPR55 played a critical role in regulation of osteoclast activity, which indicated that CBD and other GPR55 antagonists might be useful for the treatment of osteoporosis [11]. Recently, it was also found that GPR55 activation promoted cancer cell proliferation, both in cell cultures and in xenografted mice, through the increased activation of the extracellular signal-regulated kinase cascade. Therefore, GPR55 seems to be a potential new biomarker and a therapeutic target in cancer [12]. In this context, selective ligands targeting GPR55 will be needed to further understand the biological role of this receptor and possibly lead to the design of new therapeutics for these different disease states. Therefore, the knowledge of the structural features of GPR55 and its ligand binding characteristics will be beneficial for drug design and development targeting this receptor.

At present there is almost no experimental structural data for the receptor GPR55. In such cases, molecular modeling studies that build and refine homology models of the receptor and dock certain ligands into these models are the most accessible approaches to studying the 3D conformation of the receptor and binding mode of the ligands. Similar homology modeling approaches have been successfully applied to many different GPCRs [13–16]. These studies provide valuable information regarding binding modes of ligands and identifying amino acid residues that are crucial for ligand recognition. Furthermore, homology models of GPCRs have been utilized in structure-based virtual screening studies that led to novel and selective ligands [17,18].

The first high resolution template that is suitable for homology modeling of GPCRs became available in 2000 with the crystallization of bovine rhodopsin [19]. Since it was the only three dimensional GPCR structure available it has been widely used as the standard template for comparative modeling studies. These models have been used to explain binding modes and ligand–receptor interactions, rationalize mutagenesis and SAR data, and perform virtual screening of chemical databases [20,21]. The crystal structures of β_2-adrenergic receptor bound to partial inverse agonist carazolol, was obtained in 2007 using two different methods to stabilize the receptor protein [22,23]. In the following year, a 2.5 Å crystal structure of the squid rhodopsin became available [24]. Later crystal structures of a turkey β_1-adrenergic receptor [25] and the human A_{2A} adenosine receptor [26] were reported. The first crystal structure of an active state GPCR was obtained in 2008 in the form of opsin, activated rhodopsin, at 2.9 Å resolution [27,28]. The number of GPCR structural templates was further increased with the crystal structures of dopamine D_3 receptor and $CXCR_4$ chemokine receptor, both crystallized by utilizing the T4-lysozyme strategy, thus validating the general applicability of this crystallization approach toward different GPCRs [29,30]. Finally, the most recently reported crystal structures of GPCRs included that of the nanobody-stabilized active state of β_2-adrenergic receptor bound to high-affinity agonist BI-167107. When compared to the inactive β_2 structure, the activated β_2 structure shows minor structural rearrangements in the ligand-binding site, while more significant changes occur at the cytoplasmic side of the receptor [31]. Other new crystal structures included those of the three opioid receptors [32–34]. These receptors all bound to their selective antagonists in the crystals.

In this study, a homology model of GPR55 was built using the adenosine A_{2A} crystal structure as the structural template. A series of ligands reported to interact with GPR55 were docked into the comparative model in order to investigate the binding site of GPR55, receptor–ligand interactions, the amino acid residues involved in binding, and to facilitate the understanding of the putative pharmacological profile of the receptor.

2. Materials and methods

2.1. Modeling platform

All computations were performed on SGI Octane 2 workstations (Silicon Graphics Inc., Mountain View, CA) running Red Hat Enterprise Linux Workstation 4 (RHEL-WS4).

2.2. Sequence alignment

The primary amino acid sequences were retrieved from the UniProt database at http://www.uniprot.org (bovine rhodopsin, P02699; β_2-adrenoceptor, P07550; GPR35, Q9HC97; LPA_4, Q99677; LPA_5, Q9H1C0; LPA_6, P43657; A_{2A} adenosine receptor, P29274; chemokine receptor CXCR4, P61073; mu opioid receptor, P42866; delta opioid receptor, P32300; kappa opioid receptor, P41145; GPR55, Q9Y2T6). The primary pairwise alignment was conducted using uniprot.com by adopting default parameters. The multiple sequence alignment of the above GPCRs was carried out using the program ClustalX 2.0.12 [35] with varied parameters while the default ones seemed to be the optimal for our target proteins. Manual adjustments were made to the final pairwise alignment in order to properly align the cysteine residues that form a disulfide bridge that tethers the EL2 loop to the top portion of TM3 and to place gaps in structurally nonconserved regions. This was achieved by sliding the sequences and removing gaps where necessary.

2.3. Homology modeling

The homology modeling template was obtained from the PDB Data Bank at http://www.pdb.org (PDB code = 3EML, 2.6 Å AA_2AR). The 3D models of GPR55 were constructed automatically by using the program MODELLER [36]. Using the sequence alignment and the crystal structure of the template protein as an input, MODELLER extracts large number of spatial restraints from the template structure and builds a homology model of the target protein. In total, 100 comparative models of GPR55 were generated with differing geometric conformations. The residues comprising GPR55 N-terminus (Met1-Asn16) and the C-terminus (Leu311-Gly319) were not modeled because the corresponding residues were not crystallized in the template structure. In addition, the IL3 loop of GPR55 was replaced with a poly Glycine chain of 5 residues, since the template structure contained T4-lysozyme in place of IL3.

2.4. Small molecule construction

All ten ligands used in the docking study were built with standard bond lengths and angles using the molecular modeling package SYBYL 8.1 [37]. The small molecules were assigned Gasteiger–Huckel charges and energy minimized with the Tripos Force Field (TFF).

2.5. Homology model screening, selection and optimization

Five representative cannabinoid ligands that were reported to bind GPR55 were docked into all 100 homology models generated by MODELLER using GOLD 4.1 [38]. The docked GOLD score for all 5 compounds of 100 models were analyzed (see Supporting Information). Based on the overall GOLD fitness score, model number 16 was chosen due to the fact that it showed the highest score for CBD, and reasonably good score for 2-arachidonoyl LPI. Also for the other three ligands, they produce above average scores as well. Two top scored receptor models for 2-arachidonoyl-LPI were not chosen due to the fact that the docking poses of the ligand were inverted. In those receptor models the ligand 2-arachidonoyl LPI adopted an unfavorable docking pose in which the polar head group

Table 1
Sequence comparison of GPR55 with the bovine rhodopsin, the human β_2 adrenergic receptor, and the human adenosine A_{2A} receptor.

Domain	Bovine rhodopsin		β_2-Adrenoceptor		A_{2A} adenosine receptor	
	Identity (%)[a]	Similarity (%)[b]	Identity (%)[a]	Similarity (%)[b]	Identity (%)[a]	Similarity (%)[b]
TM1	17	55	14	35	21	45
TM2	26	48	26	48	33	67
TM3	9	50	26	56	33	67
TM4	13	44	13	39	26	44
TM5	16	48	23	43	13	32
TM6	17	34	6	31	6	34
TM7	12	44	18	45	20	60
EL1	0	0	0	33	0	0
EL2	17	28	14	33	5	19
EL3	0	29	0	33	0	21
IL1	17	33	17	50	0	17
IL2	22	44	10	20	20	20
IL3	0	29	0	37	0	43
N terminal	0	17	6	44	0	50
C terminal	14	43	11	28	25	43
Entire protein	14	41	14	39	18	42

[a] Percent identity.
[b] Percent similarity, as determined by ClustalX 2.0.12. Two amino acids are considered to be similar if they are identical or if they are both members of the same structure strongly conserved group.

was placed deep in the binding pocket while the nonpolar tail was pointing up toward the solvent exposed extracellular region of the receptor as opposed to being placed deeper in the ligand binding site. In order to produce an energetically reasonable conformation the model was energy minimized with the backbone constrained using the TFF. Gasteiger–Huckel charges were assigned and dielectric constant of 4.0 was employed. The minimization was run until the number of iterations exceeded 100,000 or when the energy gradient fell below 0.05 kcal/(mol × Å). The stereochemical quality of the model was assessed using PROCHECK [39] and MolProbity [40].

2.6. Docking studies

The ten ligands (including the five applied during model screening process) that were used in this study were docked into the GPR55 model using GOLD 4.1. For the docking study, the binding site of the receptor was defined to be all atoms within 15 Å radius of oxygen atom on Tyr101. The compounds were docked twenty times each with standard GOLD parameters and the default GOLD scoring was used. For all the ligands the best GOLD-docked solutions were selected and merged into the GPR55 receptor. The combined receptor–ligand structures were energy-minimized following the method described above. The minimization step optimized the interaction between ligands and the GPR55 homology model by removing clashes and lowering strain energy.

3. Results and discussion

3.1. Sequence analysis

Although, initially thought to be a new cannabinoid receptor, GPR55 shares a relatively low amino acid sequence identity to CB1 (13.5%) and CB2 (14.4%). Interestingly, GPR55 was found to have about 30% sequence identity to lysophosphatidic acid receptor 5 (LPA_5), 30% with LPA_4, 29% with LPA_6, and 37% with another orphan receptor GPR35 [8]. In order to identify a suitable template for homology modeling operation of GPR55, database search was performed using the basic local alignment search tool (BLAST). From all the crystal structures of GPCRs that were available at the time of this study, human A_{2A} adenosine receptor had the highest sequence identity to GPR55. Also the fact that LPA_4, LPA_6, and A_{2A} adenosine receptor all belong to the same purinergic receptor sub-family of GPCRs makes crystal structure of A_{2A} adenosine receptor a viable choice as the template for homology modeling. One of the most important steps in homology modeling study is the sequence alignment between the target and the template amino acid sequence. The multiple sequence alignment was accomplished using the program ClustalX and it included the sequences of GPCRs that are closely related to GPR55 (LPA_4, LPA_5, LPA_6, GPR35), bovine rhodopsin, β_2 adrenergic receptor, and the template A_{2A} adenosine receptor (Fig. 1). The resulting sequence alignment showed that GPR55 structure contained most of the highly conserved residues that were found in class A GPCRs with the exception of proline residue at position 7.50 [41]. Interestingly, the conserved 'CWXP' motif of TM6 found in most GPCRs was replaced by the amino acid residues 'SFLP' in GPR55. While bovine rhodopsin, β_2 adrenergic, and adenosine A_{2A} sequences contained the conserved 'N(7.49)PxxY(7.53)' motif in the TM7, the GPR55 sequence had 'D(7.49)VxxY(7.53)' one within the same domain. It was interesting to note that Asn of 'NPxxY' motif was also replaced with Asp in the LPA receptors and GPR35. The two conserved Cys residues C(3.25) and C(xl2.50), which form a disulfide linkage that tethers the top of TM3 to EL2 in many GPCRs, were both present in the GPR55 structure.

The sequence identity of GPR55 was compared to several other crystallized GPCRs by domain and this data is presented in Table 1. Overall, GPR55 shares 18% sequence identity and 42% sequence similarity to the human adenosine A_{2A} receptor. Within the more structurally conserved transmembrane regions, the sequence identity is 22% and the amino acid sequence similarity is 50%. Recently the crystal structure of the CXCR4 receptor and opioid receptors were solved. Similar multiple sequence alignment of GPR55 and CXCR4 followed by a pairwise alignment showed that GPR55 and CXCR4 share 21% sequence identity (See Supporting Information). Therefore CXCR4 crystal structure along with other newly available templates would be considered as other feasible template for the homology modeling studies of GPR55 in the future. On the other hand, GPR55 showed a consistent high homology to LPA receptors (LPA_4, LPA_5, and LPA_6). Since LPA_4, LPA_6 and A2A all belong to the same purinegic receptor family, while CXCR4 does not, a template from the related receptor family might provide benefit for genetic similarity purposes.

3.2. GPR55 homology model construction, optimization and validation

Based on the sequence alignment in Fig. 1, homology models of GPR55 were generated by MODELLER based on the template

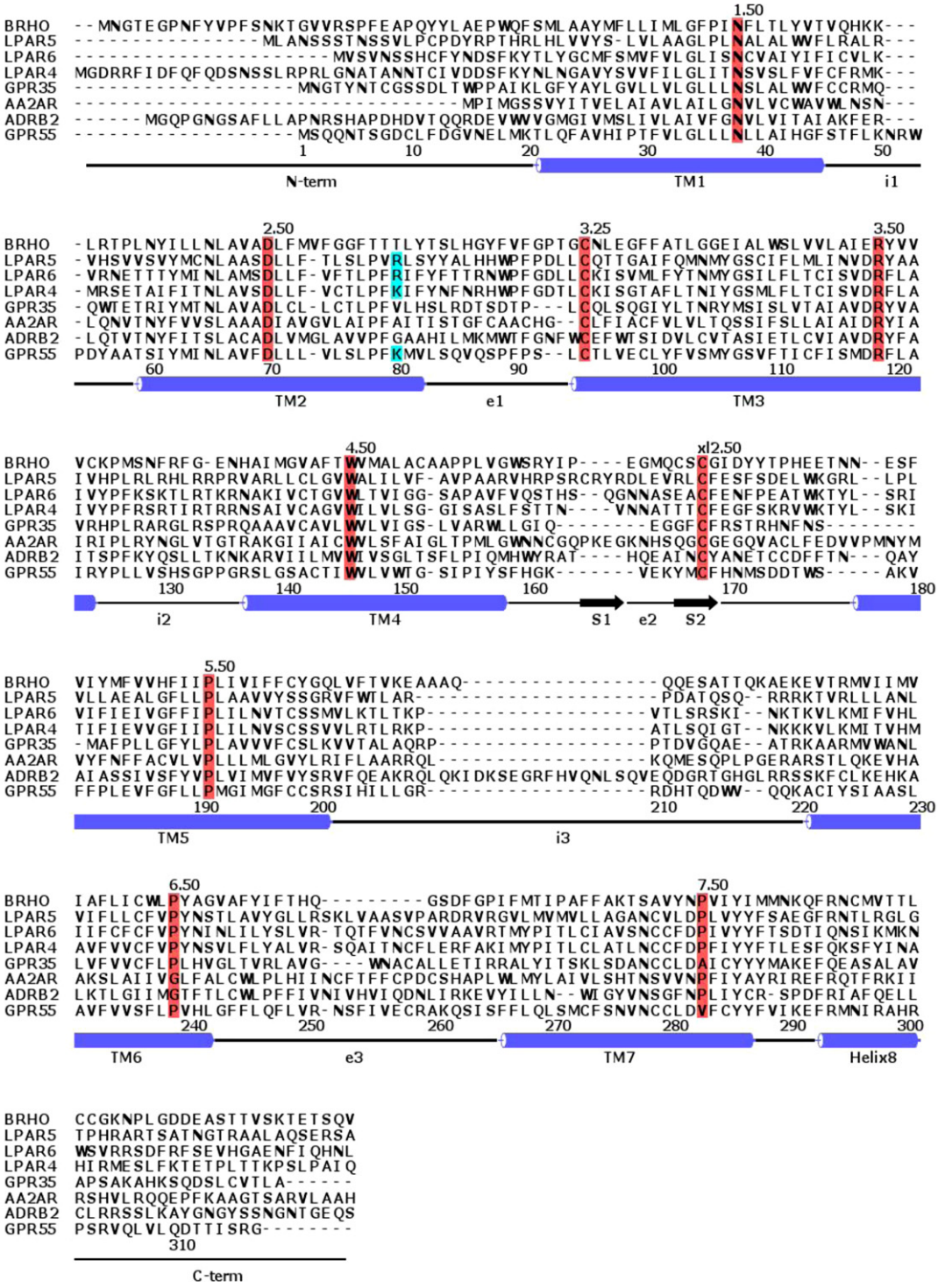

Fig. 1. Sequence alignment of bovine rhodopsin (BRHO), LPA receptor subtypes LPA_{4-6} (LPAR4–6), GPR35, human adenosine A_{2A} receptor (AA2AR), human β_2 adrenergic receptor (ADRB2), and GPR5. The Ballesteros–Weinstein numbering system was adopted to mark all the conserved amino acid residues among most of the GPCRs and colored in red. The positively charged amino acid residues that seem to be important for ligand recognition of GPR55 and LPA receptors are colored in blue. The helical range of each helix was marked in general, not a specific manner, in order to represent most of well-known GPCR structures. (For interpretation of the references to color in this figure legend, the reader is referred to the web version of the article.)

of adenosine A_{2A} crystal structure solved by Jaakola et al. at 2.6 Å resolution using the T4-lysozyme fusion strategy [26]. Out of 100 models generated, one model was chosen (see Section 2) for further energy minimization while the backbone was constrained followed by a short dynamics simulation to reach energetically favorable conformation. The overall weighted Root Mean Square Distance (RMSD) value between optimized and non-optimized models was 0.40 Å, which indicated only insignificant side chains re-orientation occurred during the optimization process. The local geometry of the optimized structure was checked using PROTABLE and PROCHECK. PROTABLE results showed that all amino acid residues had reasonable bond lengths and bond angles. The Ramachandran plot

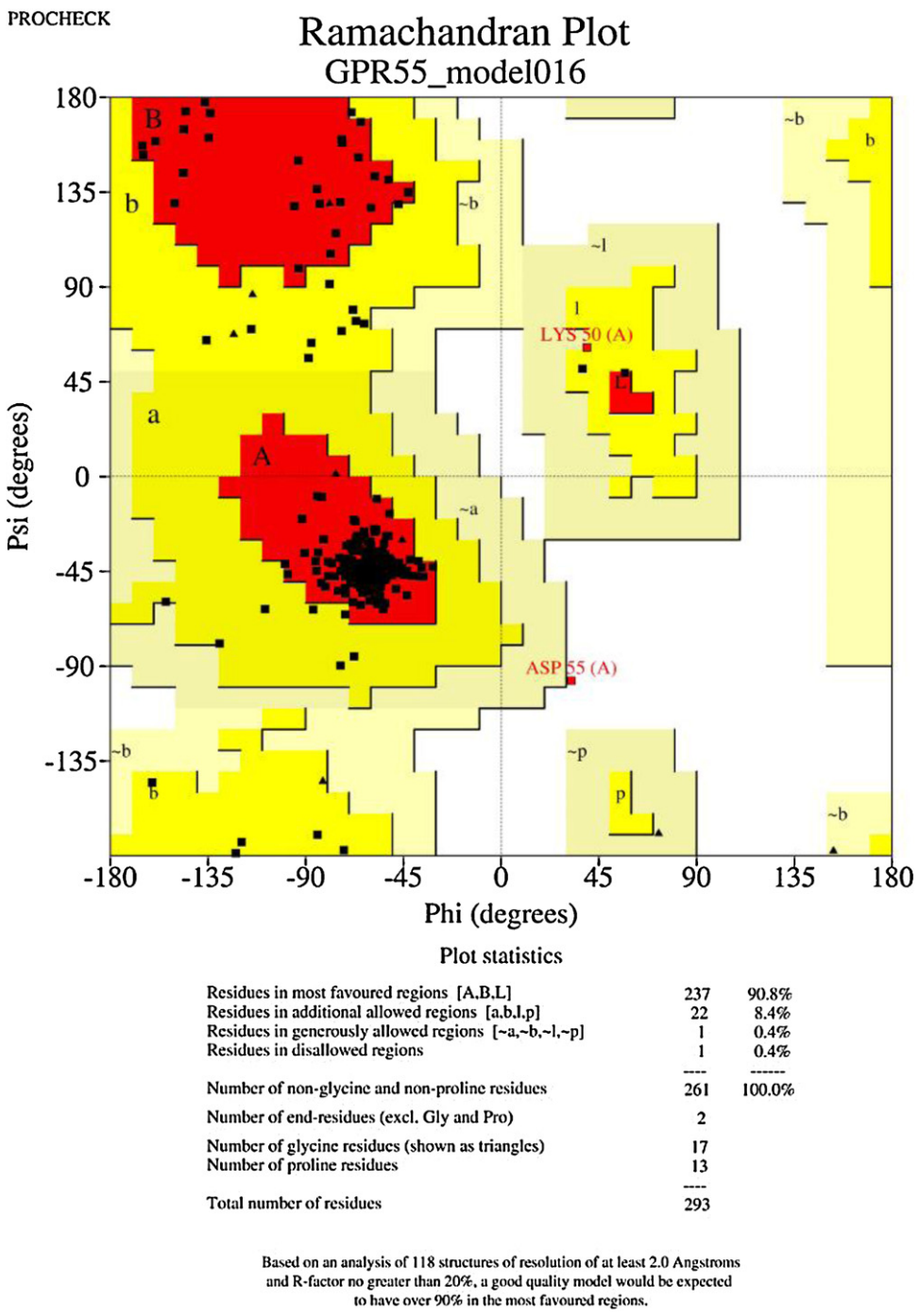

Fig. 2. Ramachandran plot of the GPR55 homology model.

obtained from PROCHECK is shown in Fig. 2. As seen from the Ramachandran plot, more than 99% of the amino acid residues were either in the most favored regions or the additionally allowed regions. The Asp55, the only residue in the disallowed region, is located on the IL-1 on the cytoplasmic side of the receptor, which was believed not to interfere with ligand binding. The stereochemical quality of the model was further verified using MolProbity. The results indicated that 95.2% of all residues were in favored regions and 98.6% of all residues were in allowed regions. The four amino acid residues that were identified as having unfavorable Phi and Psi angles were Lys50 (IL1), Arg52 (IL1), Cys260 (EL3), and Asp55 (IL1). These residues are located far from the putative binding site and should not influence ligand binding study of GPR55.

The comparison of GPR55 homology model with A_{2A} crystal structure is shown in Fig. 3. The overall weighted Root Mean Square Distance (RMSD) value between them was 3.75 Å. In the homology modeling operation, the comparative model seems always mimic the parent crystal structure and adapt most of its structural features. As such the GPR55 model is structurally very similar to A_{2A} crystal structure, albeit few differences. The TM1 domain in both structures overlapped well and adopted a straight extension. The TM2 domain in GPR55 model contained somewhat tighter coiling around the middle of the helix compared to A_{2A} structure. Both models have the same number amino acid residues in the EL1 domain and it has the similar 3D conformation in both structures. The TM3 was almost identical in both structures. The

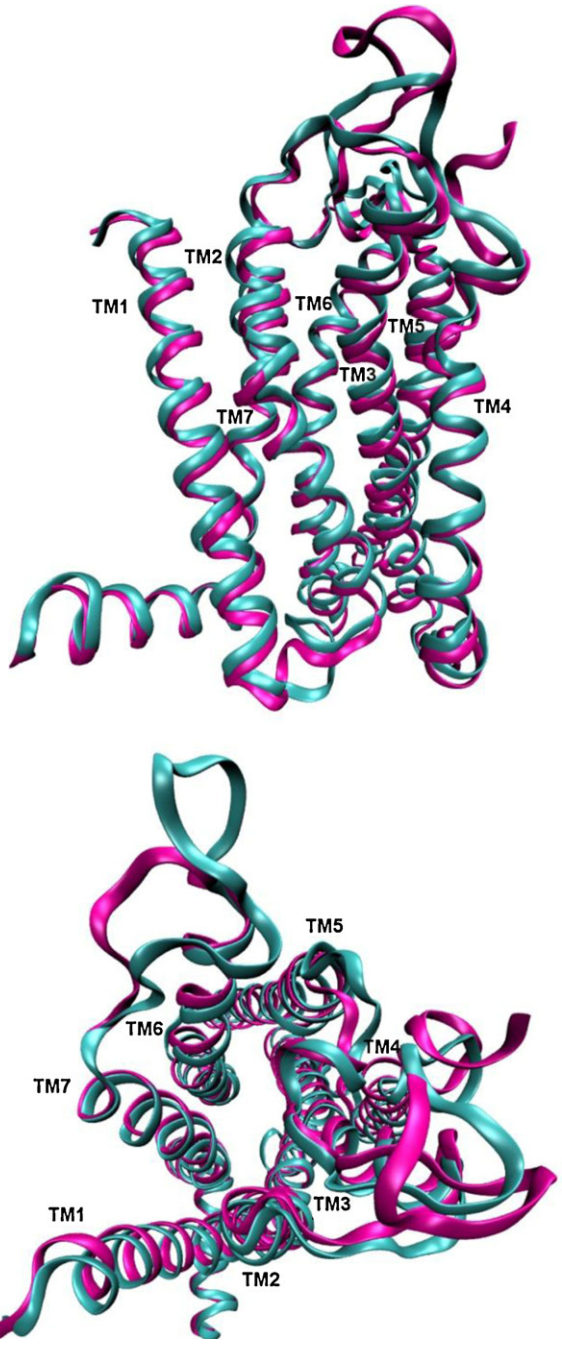

Fig. 3. Homology model of GPR55 overlapped with the template crystal structure of human adenosine A2A receptor in ribbon. The GPR55 model is presented in cyan and the adenosine A2A model is in magenta. (For interpretation of the references to color in this figure legend, the reader is referred to the web version of the article.)

A_{2A} receptor has more amino acid residues in the EL2 domain compared to GPR55 and furthermore the tip of the extracellular loop 2 was not crystallized in the A_{2A} structure. The EL2 domain is comparatively more compact and sits mostly on top of TM3 and TM4 in the GPR55 model. When compared to A_{2A} template, the top part of helix 4 in GPR55 model had tighter coiling due to a one residue gap in that region. The TM5, TM6, and TM7 domains in both models adopted the same 3D conformation. The TM6 and TM7 domains of adenosine A_{2A} receptor contained the characteristic kinks seen in the family A GPCRs, induced by highly conserved Pro residues. In the GPR55 model, TM6 had a kink in the middle of the helix that caused the top of the helix bend toward TM5. By adopting the spatial arrangements of the parent structure, TM7 of GPR55 bended slightly away from the binding site. The EL3 domain in GPR55 contains seven extra amino acid residues when compared to the template structure and it was positioned above TM6 and TM7 and it protruded slightly into the binding pocket. The two conserved Cys residues C(3.25) and C(xl2.50) were linked to form the disulfide bond from the top of TM3 to EL2 as seen in many GPCRs. Although the general 3D structures of all rhodopsin-like GPCRs were well conserved, the difference in primary amino acid sequence provided binding sites with diverse chemical features that recognized variety of selective natural and synthetic ligands.

Table 2
Top GoldScores of docked ligands.

Ligand	GoldScore	*S*(hb_ext)[a]	*S*(vdw_ext)[a]	*S*(hb_int)[a]	*S*(int)[a]
Δ^9-THC	50.16	5.86	34.89	0.00	−3.67
CP55940	49.74	6.02	41.25	0.00	−13.00
O-1602	48.80	6.00	33.69	0.00	−3.51
HU-210	33.73	5.93	26.99	0.00	−9.31
CBD	62.47	6.00	44.14	0.00	−4.23
AM-281	73.68	1.08	57.75	0.00	−6.81
JWH-015	56.90	3.97	43.48	0.00	−6.86
Anandamide	63.29	6.00	52.87	0.00	−15.40
2-AG	59.54	7.72	51.55	0.00	−19.07
2-Arachidonoyl-LPI	73.41	12.68	60.07	0.00	−21.87

[a] GoldScore components: *S*(hb_ext): protein–ligand hydrogen bond energy (external H-bond); *S*(vdw_ext): protein–ligand van der Waals energy (external vdw); *S*(hb_int): ligand intermolecular hydrogen bond energy (internal H-bond); *S*(int): ligand internal energy term.

3.3. Docking study analysis

In order to study the ligand binding characteristics of GPR55, a docking study was then performed by applying a set of small molecules shown to bind GPR55 (Fig. 4). The lowest energy conformations of all ligands used in the study were docked into the GPR55 receptor model using GOLD, a genetic algorithm-based automated docking program. The results of GOLD docking experiments are reported in Table 2 and the final conformations of the receptor–ligand representative complexes are illustrated in Fig. 5.

3.3.1. Putative universal binding pocket of GPR55

In general, the putative binding site of GPR55 was located close to the top of the transmembrane region and it was built mainly by TM2, TM3, TM6, and TM7. The ligands stayed away from the TM4 and TM5, due to protrusion of EL2. Since in the template A_{2A} crystal structure, the antagonist ZM241385 bound in an extended conformation perpendicular to the plane of the membrane, in the GPR55 comparative model all ligands were docked into the receptor in a vertical manner as well. As seen in Table 2, all small molecules had reasonable GOLD fitness scores and both hydrogen bonding and hydrophobic interactions were responsible for ligand recognition. Ryberg et al. showed that GPR55 can be activated by various cannabinoids like Δ^9-THC, CP55940, HU210, and O-1602. Cannabidiol acted as an antagonist with an IC_{50} of 440 nM. The docking study showed that these phytocannabinoid compounds (including agonists and antagonist) bound at a similar site on the GPR55 model. The hydroxyl groups of these molecules formed a hydrogen bonding interaction with Lys80 and the hydrophobic ends of the molecules were in close proximity to hydrophobic amino acid residues.

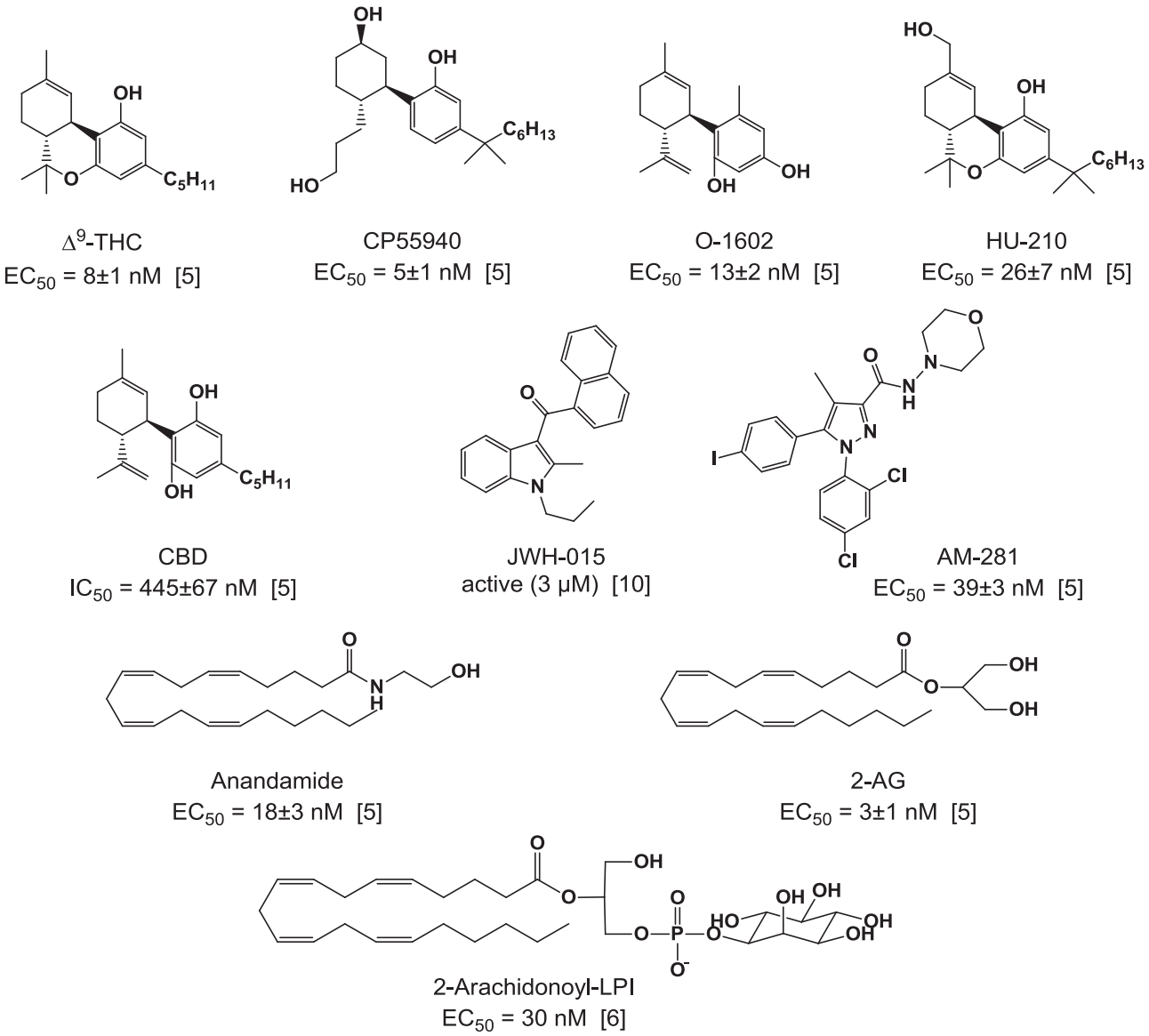

Fig. 4. Ligands used in the docking study shown with EC_{50} values for the reported agonists and the reported IC_{50} value for the antagonist CBD.

3.3.2. Hydrophobic binding domains

There seem to be two distinct hydrophobic pockets in the ligand binding site of GPR55. One of the hydrophobic pockets lay in close proximity to the top part of the ligand and it was composed of hydrophobic residues including Phe169, Leu 270, Val86, and Leu83. The second hydrophobic region was located deeper in the binding site where the long aliphatic tails of the natural ligand LPI and endogenous cannabinoids seemed to be positioned. This hydrophobic site contained amino acid residues Phe102, Tyr101, Val242, and Phe246 which seemed to stabilize the bound ligand through nonpolar interactions. While the cannabinoid compounds were mainly anchored by the hydrogen bonding involving Lys80, the hydrophobic parts of the compounds occupied the hydrophobic pockets and were stabilized by the nonpolar amino acid residues. The endocannabinoids anandamide and 2-arachidonoyl glycerol (2-AG) were also shown to activate GPR55. Within the ligand binding site of GPR55, the carbonyl moieties of these two compounds hydrogen-bonded to Lys80, while the long hydrophobic tails lay in one of the hydrophobic pockets. The highest-scoring GOLD poses of these two molecules showed the lipophilic tails to be flanked by hydrophobic amino acid residues including Tyr101, Phe102, Val242, and Phe246.

3.3.3. Putative universal anchor amino acid residue Lys80 (2.60)

As mentioned above, the amino acid residue Lys80 (2.60) was shown to interact with all the ligands that were applied for the study. As discussed earlier, GPR55 shared high homology with LPA_5 receptor. It should be noted that LPA receptors 4–6 and GPR55 all contain a positively charged amino acid (either Lys or Arg) at the 2.60 position. In case of the LPA_5 receptor this basic residue was shown to interact with the polar head group of LPA and a site-directed mutagenesis study of R2.60N mutant lead to abolished receptor activation [42]. In the GPR55 binding site, this conserved residue Lys80 hydrogen bonded to the phosphate group of 2-arachidonoyl LPI as well as other ligands. Overall, the docking studies indicated that Lys80 (2.60) seemed to be a very important anchor residue for ligand binding of GPR55.

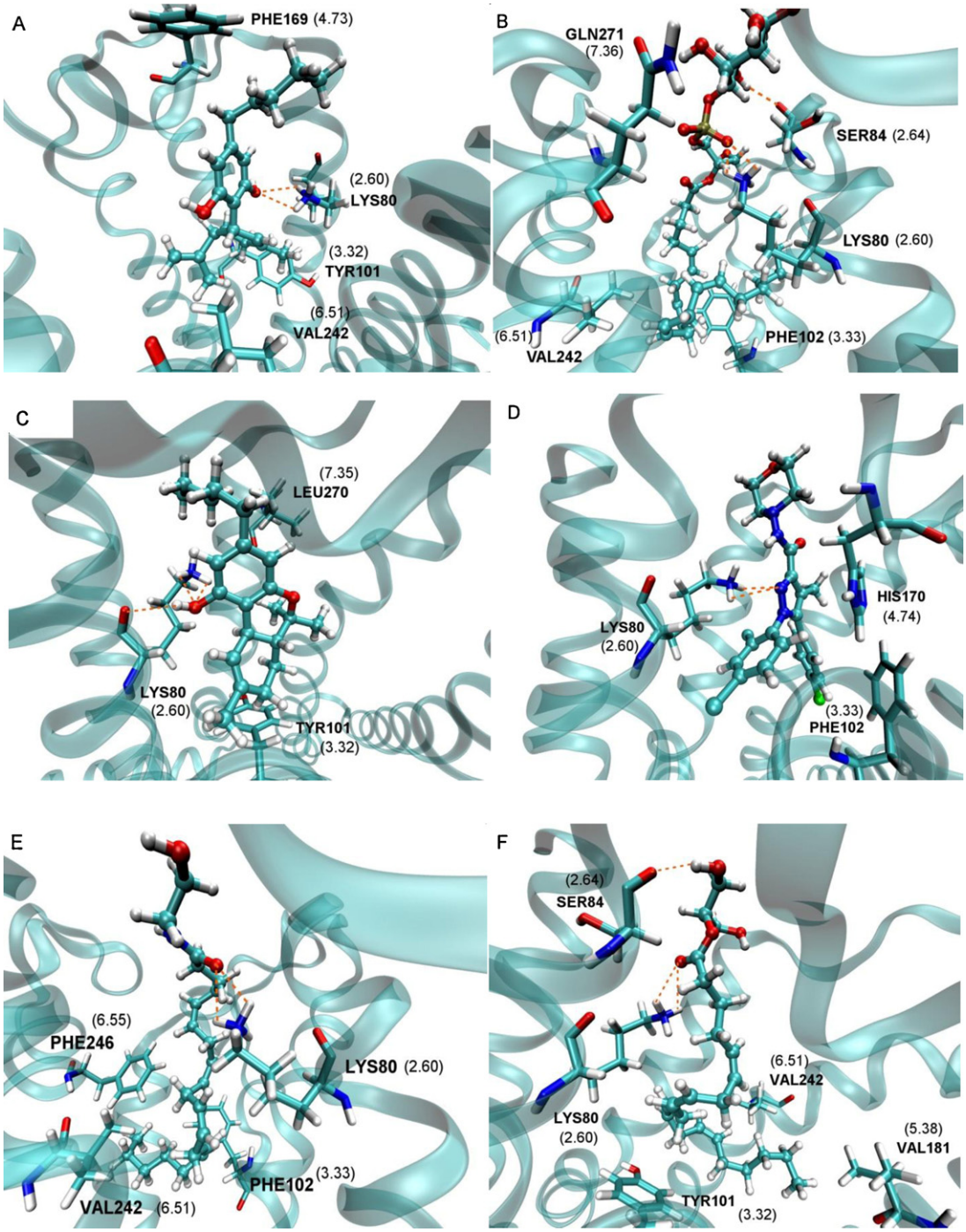

Fig. 5. The binding modes of CBD (A), 2-arachidonoyl LPI (B), Δ^9-THC (C), AM-281 (D), anandamide (E), 2-AG (F) in the homology model of GPR55.

3.3.4. Possible activation mechanism of GPR55

Despite the fact that GPCRs can be activated by a vast variety of agonists, a common activation mechanism is believed to be shared among all the family A, rhodopsin-like receptors. Over the years, many highly conserved residues have been identified in the transmembrane region that is thought to be important for the activation mechanism of GPCRs, including Trp 6.48 [43]. In the recently published agonist bound crystal structure of adenosine A_{2A}, the indole ring of Trp 6.48 was reported to move 1.9 Å to avoid a steric clash with the ribose ring of the agonist, a movement that leads to the rotation and tilt of the intracellular side of helix IV [44]. The vertical tilt of the transmembrane domain VI, combined with the movement of helix V and an axial shift of helix III were thought to open a G-protein binding site on the intracellular surface of the 7TM receptor. This particular Trp residue corresponds to the residue of Phe239 in the GPR55 binding site. Further analysis of our docking results showed that the GPR55 agonist 2-arachidonoyl LPI bound the receptor in such a way that brings its hydrophobic tail in close proximity to potentially interact with Phe239. On the other hand, GPR55 antagonist CBD binds further away from this amino acid residue (Fig. 6). In the docked pose, the closest distance between the center of the phenyl ring of Phe239 and the aliphatic tailing carbon atom of 2-arachidonoyl LPI was found to be 5.02 Å while the CBD was 7.15 Å away. These findings seemed to be in line with the putative pharmacological profile of these two ligands. Due to the fact that current homology model was constructed

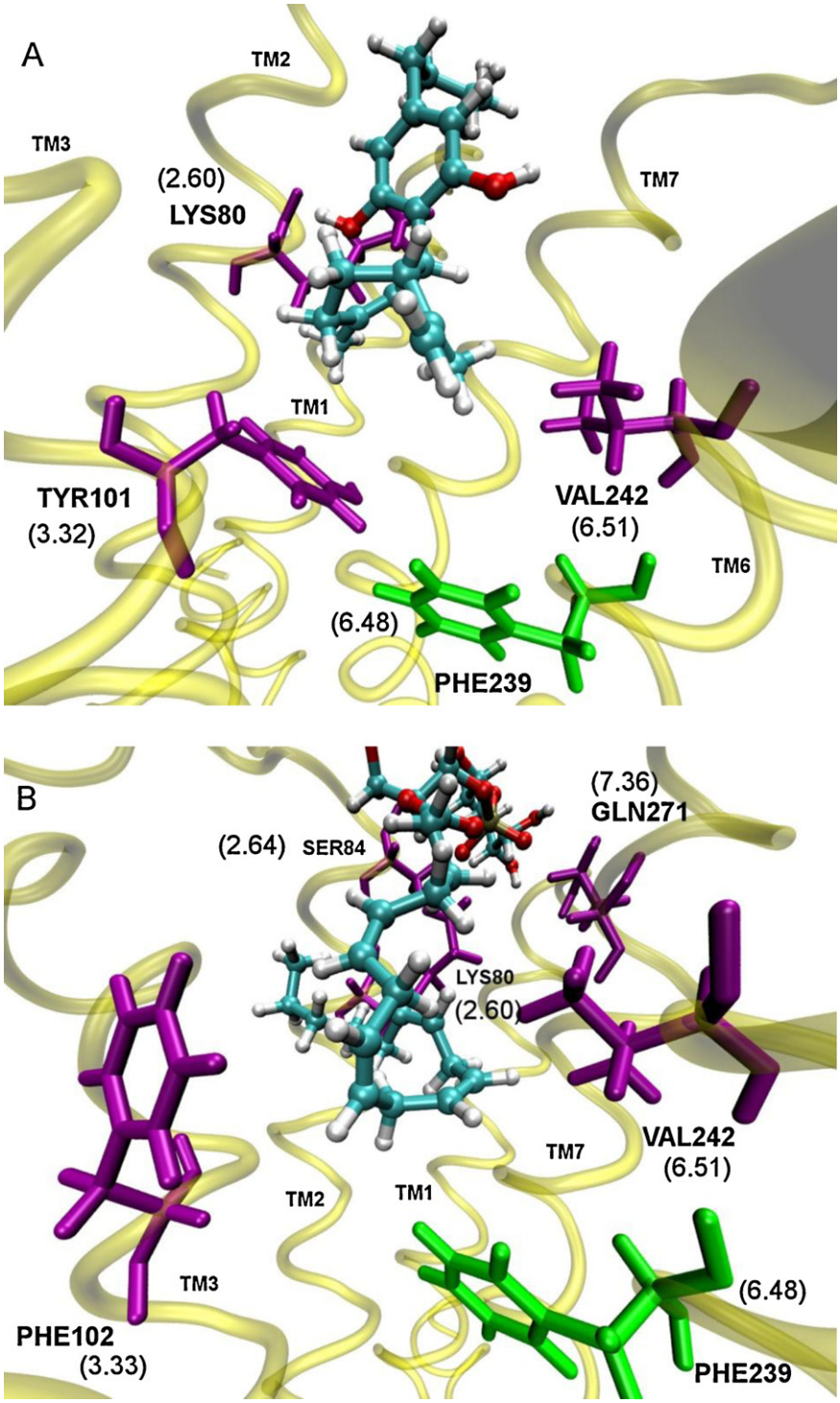

Fig. 6. Comparison of binding modes of GPR55 antagonist CBD (A) and agonist 2-arachidonoyl LPI (B). Amino acid residues that are found to be important for GPR55 ligand recognition is shown in purple. Phe239 which is thought to be involved in GPR55 activation is colored in green.

based on the antagonist bound crystal structure of adenosine A_{2A} receptor, such observation would serve as a clue for the future comparative homology modeling of GPR5 based on the agonist bound crystal structure of the adenosine A_{2A} receptor.

4. Conclusion

The homology model of GPR55 was built based on the crystal structure of adenosine A_{2A} receptor. The model was optimized and validated using various methods. A number of compounds reported to act as GPR55 ligands were docked into the resulted homology model and the ligand–protein complexes have been analyzed. Based on the docking results, it seemed that most of the ligands bound into a common upper-transmembrane domain of the GPR55 model while both hydrogen bonding and hydrophobic interactions contributed to the ligand recognition. The docking results indicated that the amino acid residue Lys80 seemed to be essential in GPR55 ligand recognition through a critical hydrogen bonding interaction with the docked ligands. This observation was in line with the fact that its corresponding conserved amino acid residue in the LPA_5

receptor, which is Arg78 (2.60), had been confirmed to be critical for its ligand binding and activation of the receptor. In the absence of any structural data regarding GPR55, this might serve as an indirect validation of the GPR55 comparative model. GPR55 is an intriguing therapeutic target and the development of selective compounds targeting GPR55 will be of great value in answering these outstanding questions regarding its pharmacology and physiological role in the body. The molecular modeling work presented here may serve as a starting point to understand the putative pharmacological profile of GPR55, to characterize the new ligands [45,46] interaction with the receptor, and to facilitate the design of selective ligands in recognition of the receptor.

Acknowledgement

The work was partially supported by PHS grant DA 24022 from NIDA (YZ).

Appendix A. Supplementary data

Supplementary data associated with this article can be found, in the online version, at http://dx.doi.org/10.1016/j.jmgm.2012.10.005.

References

[1] D. Filmore, It's a GPCR world, Modern Drug Discovery 7 (2004) 24–26.
[2] M. Sawzdargo, T. Nguyen, D.K. Lee, K.R. Lynch, R. Cheng, H.H.Q. Heng, S.R. George, B.F. O'Dowd, Identification and cloning of three novel human G protein-coupled receptor genes GPR52, ψGPR53 and GPR55: GPR55 is extensively expressed in human brain, Molecular Brain Research 64 (1999) 193–198.
[3] A.J. Brown, Novel cannabinoid receptors, British Journal of Pharmacology 152 (2007) 567–575.
[4] H. Sharir, M.E. Abood, Pharmacological characterization of GPR55, a putative cannabinoid receptor, Pharmacology & Therapeutics 126 (2010) 301–313.
[5] E. Ryberg, N. Larsson, S. Sjoegren, S. Hjorth, N.O. Hermansson, J. Leonova, T. Elebring, K. Nilsson, T. Drmota, P.J. Greasley, The orphan receptor GPR55 is a novel cannabinoid receptor, British Journal of Pharmacology 152 (2007) 1092–1101.
[6] S. Oka, T. Toshida, K. Maruyama, K. Nakajima, A. Yamashita, T. Sugiura, 2-Arachidonoyl-*sn*-glycero-3-phosphoinositol: a possible natural ligand for GPR55, Journal of Biochemistry 145 (2008) 13–20.
[7] R.A. Ross, The enigmatic pharmacology of GPR55, Trends in Pharmacological Sciences 30 (2008) 156–163.
[8] A. Moriconi, I. Cerbara, M. Maccarrone, A. Topai, GPR55: current knowledge and future perspective of a purported "Type-3" cannabinoid receptor, Current Medicinal Chemistry 17 (2010) 1411–1429.
[9] P.C. Staton, J.P. Hatcher, D.J. Walker, A.D. Morrison, E.M. Shapland, J.P. Hughes, E. Chong, P.K. Mander, P.J. Green, A. Billinton, M. Fulleylove, H.C. Lancaster, J.C. Smith, L.T. Bailey, A. Wise, A.J. Brown, J.C. Richardson, I.P. Chessell, The putative cannabinoid receptor GPR55 plays a role in mechanical hyperalgesia associated with inflammatory and neuropathic pain, Pain 139 (2008) 225–236.
[10] J.E. Lauckner, J.B. Jensen, H. Chen, H. Lu, B. Hille, K. Mackie, GPR55 is a cannabinoid receptor that increases intracellular calcium and inhibits M current, Proceedings of the National Academy of Sciences of the United States of America 105 (2008) 2699–2704.
[11] L.S. Whyte, E. Ryberg, N.A. Sims, S.A. Ridge, K. Mackie, P.J. Greasley, R.A. Ross, M.J. Rogers, The putative cannabinoid receptor GPR55 affects osteoclast function in vitro and bone mass in vivo, Proceedings of the National Academy of Sciences of the United States of America 106 (2009) 16511–16516.
[12] C. Andradas, M. Caffarel, E. Perez-Gomez, M. Salazar, M. Lorente, G. Velasco, M. Guzman, C. Sanchez, The orphan G-protein coupled receptor GPR55 promotes cancer cell proliferation via ERK, Oncogene 30 (2010) 245–252.
[13] J.A. Ballesteros, L. Shi, J.A. Javitch, Structural mimicry in G protein-coupled receptors: implications of the high-resolution structure of rhodopsin for structure–function analysis of rhodopsin-like receptors, Molecular Pharmacology 60 (2001) 1–19.
[14] O.M. Becker, S. Shacham, Y. Marantz, S. Noiman, Modeling the 3D structure of GPCRs: advances and application to drug discovery, Current Opinion in Drug Discovery & Development 6 (2003) 353–361.
[15] M. Nowak, M. Kolaczkowski, M. Pawlowski, A.J. Bojarski, Homology modeling of the serotonin 5-HT_1A receptor using automated docking of bioactive compounds with defined geometry, Journal of Medicinal Chemistry 49 (2006) 205–214.
[16] G. Li, K.M. Haney, G.E. Kellogg, Y. Zhang, Comparative docking study of anibamine as the first natural product CCR5 antagonist in CCR5 homology models, Journal of Chemical Information and Modeling 49 (2009) 120–132.
[17] A. Evers, T. Klabunde, Structure-based drug discovery using GPCR homology modeling: successful virtual screening for antagonist of the alpha1A adrenergic receptor, Journal of Medicinal Chemistry 48 (2005) 1088–1097.
[18] O.M.H Salo, K.H. Raitio, J.R. Savinainen, T. Nevalainen, M. Lahtela-Kakkonen, J.T. Laitinen, T. Jarvinen, A. Poso, Virtual screening of novel CB2 ligands using a comparative model of the human cannabinoid CB2 receptor, Journal of Medicinal Chemistry 48 (2005) 7166–7171.
[19] K. Palczewski, T. Kumasaka, T. Hori, C.A. Behnke, H. Motoshima, B.A. Fox, I. Le Trong, D.C. Teller, T. Okada, R.E. Stenkamp, M. Yamamoto, M. Miyano, Crystal structure of rhodopsin: a G protein-coupled receptor, Science 289 (2000) 739–745.
[20] A. Patny, P.V. Desai, M.A. Avery, Homology modeling of G-protein coupled receptors and implications in drug design, Current Medicinal Chemistry 13 (2006) 1667–1691.
[21] C. Bizzantz, P. Bernard, M. Hibert, D. Rognan, Protein-based virtual screening of chemical databases. II. Are homology models of G-protein coupled receptors suitable targets? Proteins: Structure, Function and Bioinformatics 50 (2003) 5–25.
[22] S.G.F. Rasmussen, H.-J. Choi, D.M. Rosenbaum, T.S. Kobilka, F.S. Thian, P.C. Edwards, M. Burghammer, V.R.P. Ratnala, R. Sanishvili, R.F. Fischetti, G.F.X. Schertler, W.I. Weis, B.K. Kobilka, Crystal structure of the human β2 adrenergic G-protein-coupled receptor, Nature 450 (2007) 383–387.
[23] V. Cherezov, D.M. Rosenbaum, M.A. Hanson, S.G.F. Rasmussen, F.S. Thian, T.S. Kobilka, H.J. Choi, P. Kuhn, W.I. Weis, B.K. Kobilka, R.C. Stevens, High-resolution crystal structure of an engineered human beta2-adrenergic G protein-coupled receptor, Science 318 (2007) 1258–1265.
[24] M. Murakami, T. Kouyama, Crystal structure of squid rhodopsin, Nature 453 (2008) 363–367.
[25] T. Warne, M.J. Serrano-Vega, J.G. Baker, R. Moukhametzianov, P.C. Edwards, R. Henderson, A.G.W. Leslie, C.G. Tate, G.F. Schertler, Structure of a β_1-adrenergic G-protein-coupled receptor, Nature 454 (2008) 486–492.
[26] V.-P. Jaakola, M.T. Griffith, M.A. Hanson, V. Cherezov, E.Y.T. Chien, J.R. Lane, A.P. Izjerman, R.C. Stevens, The 2.6 Angstrom crystal structure of a human A_{2A} adenosine receptor bound to an antagonist, Science 322 (2008) 1211–1217.
[27] P. Scheerer, J.H. Park, P.W. Hildebrand, Y.J. Kim, N. Krauss, H.W. Choe, K.P. Hofmann, O.P. Ernst, Crystal structure of opsin in G-protein-interacting conformation, Nature 455 (2008) 497–502.
[28] J.H. Park, P. Scheerer, K.P. Hofmann, H.W. Choe, O.P. Ernst, Crystal structure of the ligand-free G-protein-coupled receptor opsin, Nature 454 (2008) 183–187.
[29] E.Y.T. Chien, W. Liu, Q. Zhao, V. Katritch, G.W. Han, M.A. Hanson, L. Shi, A.H. Newman, J.A. Javitch, V. Cherezov, R.C. Stevens, Structure of the human dopamine D3 receptor in complex with a D2/D3 selective antagonist, Science 330 (2010) 1091–1095.
[30] B. Wu, E.Y.T. Chien, C.D. Mol, G. Fenalti, W. Liu, V. Katritch, R. Abagyan, A. Brooun, P. Wells, F.C. Bi, D.J. Hamel, P. Kuhn, T.M. Handel, V. Cherezov, R.C. Stevens, Structures of the CXCR4 chemokine GPCR with small-molecule and cyclic peptide antagonists, Science 330 (2010) 1066–1071.
[31] S.G.F. Rasmussen, H.-J. Choi, J.J. Fung, E. Pardon, P. Casarosa, P.S. Chae, B.T. DeVree, D.M. Rosenbaum, F.S. Thian, T.S. Kobilka, A. Schnapp, I. Konetzki, R.K. Sunahara, S.H. Gellman, A. Pautsch, J. Steyart, W.I. Weis, B.K. Kobilka, Structure of a nanobody-stabilized active state of the β_2 adrenoceptor, Nature 469 (2011) 175–180.
[32] A. Manglik, A.C. Kruse, T.S. Kobilka, F.S. Thian, J.M. Mathiesen, R.K. Sunahara, L. Pardo, W.I. Weis, B.K. Kobilka, S. Granier, Crystal structure of the μ-opioid receptor bound to a morphinan antagonist, Nature 485 (2012) 321–326.
[33] H. Wu, D. Wacker, M. Mileni, V. Katritch, G.W. Han, E. Vardy, W. Liu, A.A. Thompson, X.P. Huang, F.I. Carroll, S.W. Mascarella, R.B. Westkaemper, P.D. Mosier, B.L. Roth, V. Cherezov, R.C. Stevens, Structure of the human κ-opioid receptor in complex with JDTic, Nature 485 (2012) 327–332.
[34] S. Granier, A. Manglik, A.C. Kruse, T.S. Kobilka, F.S. Thian, W.I. Weis, B.K. Kobilka, Structure of the δ-opioid receptor bound to naltrindole, Nature 485 (2012) 400–404.
[35] M.A. Larkin, G. Blackshields, N.P. Brown, R. Chenna, P.A. McGettigan, H. McWilliam, F. Valentin, I.M. Wallace, A. Wilm, R. Lopez, J.D. Thompson, T.J. Gibson, D.G. Higgins, Clustal W and Clustal X version 2.0, Bioinformatics 23 (2007) 2947–2948.
[36] A. Sali, T.L. Blundell, Comparative protein modeling by satisfaction of spatial restraints, Journal of Molecular Biology 234 (1993) 779–815.
[37] SYBYL 8.1, Tripos International, St. Louis, MO, USA, 2009.
[38] G. Jones, P. Willett, R.C. Glen, A.R. Leach, R. Taylor, Development and validation of a genetic algorithm for flexible docking, Journal of Molecular Biology 267 (1997) 727–748.
[39] R.A. Laskowski, M.W. MacArthur, D.S. Moss, J.M. Thornton, PROCHECK: a program to check the stereochemical quality of protein structures, Journal of Applied Crystallography 26 (1993) 283–291.
[40] V.B. Chen, W.B. Arendall III, J.J. Headd, D.A. Keedy, R.M. Immormino, G.J. Kapral, L.W. Murray, J.S. Richardson, D.C. Richardson, MolProbity: all-atom structure validation for macromolecular crystallography, Acta Crystallographica D66 (2010) 12–21.
[41] J.A. Ballesteros, H. Weinstein, Integrated methods for the construction of three-dimensional models and computational probing of structure–function relations in G protein-coupled receptors, Methods in Neurosciences 25 (1995) 366–428.

[42] J.R. Williams, A.L. Khandoga, P. Goyal, J.I. Fells, D.H. Perygin, W. Siess, A.L. Parrill, G. Tigyi, Y. Fujiwara, Unique ligand selectivity of the GPR92/LPA_5 lysophosphatidate receptor indicates role in human platelet activation, Journal of Biological Chemistry 284 (2009) 17304–17319.
[43] R. Nygaard, T.M. Frimurer, B. Holst, M.M. Rosenkilde, T.W. Schwartz, Ligand binding and micro-switches in 7TM receptor structures, Trends in Pharmacological Sciences 30 (2009) 249–259.
[44] F. Xu, H. Wu, V. Katritch, G.W. Han, K.A. Jacobson, Z. Gao, V. Cherezov, R.C. Stevens, Structure of an agonist-bound human A_{2A} adenosine receptor, Science 332 (2011) 322–327.
[45] A.J. Brown, D.A. Daniels, M. Kassim, S. Brown, C.P. Haslam, V.R. Terrell, J. Brown, P.L. Nichols, P.C. Staton, A. Wise, S.J. Dowell, Pharmacology of GPR55 in yeast and identification of GSK494581A as a mixed-activity glycine transporter subtype 1 inhibitor and GPR55 agonist, Journal of Pharmacology and Experimental Therapeutics 337 (2011) 236–246.
[46] E. Kotsikorou, K.E. Madrigal, D.P. Hurst, H. Sharir, D.L. Lynch, S. Heynen-Genel, L.B. Milan, T.D. Chung, H.H. Seltzman, Y. Bai, M.G. Caron, L. Barak, M.E. Abood, P.H. Reggio, Identification of the GPR55 agonist binding site using a novel set of high-potency GPR55 selective ligands, Biochemistry 50 (2011) 5633–5647.